

Engineering Glucose Swelling Responses in Poly(*N*-isopropylacrylamide)-Based Microgels

Todd Hoare* and Robert Pelton

Department of Chemical Engineering, McMaster University, 1280 Main St. W., Hamilton, Ontario, Canada L8S 4L7

Received September 28, 2006; Revised Manuscript Received November 25, 2006

ABSTRACT: Poly(*N*-isopropylacrylamide) (PNIPAM) microgels are functionalized with aminophenylboronic acid (APBA) to produce nanoparticles which swell in response to increases in the glucose concentration. A “graft-to” approach was used to synthesize a range of microgels with different physical properties from the same base microgel. Higher APBA graft yields are achieved as the $-\text{COOH}$ groups in the platform microgel become more localized on the surface and more highly spaced within the subchains. The glucose swelling response of the graft microgels is enhanced as the PBA functional groups become more localized in the outer shell of the microgel and more randomly distributed within the gel network subchains. The glucose-induced VPTT shift observed in the PBA–microgel conjugates can be exploited to produce microgels that exhibit on–off glucose swelling as a function of temperature or enhanced swelling responses over specific glucose concentration ranges at a single, tunable temperature. The “secondary” thermal phase transition is thus applied to effect an order-of-magnitude enhancement or suppression of the “primary” glucose-induced phase transition. Both linear and nonlinear microgel glucose sensors are subsequently designed which are active within targeted glucose concentration ranges.

Introduction

Microgels that respond to a wide range of physical stimuli have been reported in the literature. Of particular interest are microgels based on poly(*N*-isopropylacrylamide) (PNIPAM) that exhibit reversible deswelling phase transitions as the temperature is increased. Functional groups can be incorporated into these microgels via copolymerization to shift the phase transition temperature and/or introduce responsiveness to other physical variables (i.e., pH or ionic strength). However, microgels that exhibit a “smart” swelling response to changes in their chemical environment would also be useful in many applications. Chemosensitive microgels may be applied as sensor units for detecting the concentration of a specific chemical in the microgel environment and/or as self-regulated release matrices for controlling the release rate of a drug according to the concentration of a particular antigen or target chemical in the gel environment. Glucose is a particularly interesting target molecule. A glucose-responsive microgel may be able both to quantify glucose concentrations in complex physiological mixtures and to regulate the in-vivo delivery of insulin for diabetic patients, reducing the frequency of insulin injections and minimizing the risk of insulin overdose and hypoglycemia.

Enzymes (i.e., glucose oxidase)¹ and lectins (i.e., concanavalin A)² have been used to generate glucose-specific swelling responses in hydrogels. However, these and other biomolecule-based approaches are strongly limited by the toxicity, instability, and potential antigenicity of enzymes and lectins in vivo. As a result, growing attention has focused on the use of phenylboronic acid (PBA) functional groups in the design of glucose-responsive polymers. The interaction between phenylboronic acids and carbohydrates was first recognized in 1874³ and was identified mechanistically in the 1940s⁴ as a reversible covalent interaction between the ionic boronate state of PBA and the *cis*-diol groups on polyols. This binding mechanism is illustrated in Figure 1.

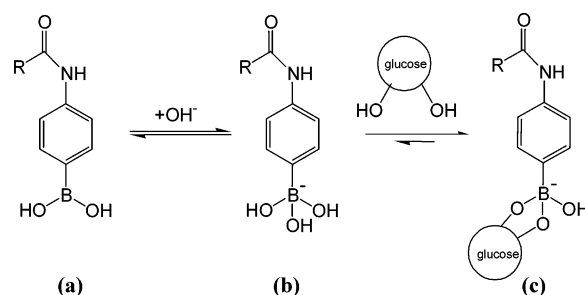


Figure 1. Reversible binding of glucose to (alkylamido)phenylboronic acids.

PBA moieties have been incorporated into a range of linear polymers, colloidal particles, polyelectrolyte complexes, and bulk hydrogels. PBA functionalization is typically achieved the copolymerization of PBA-containing vinylic monomers^{5–13} or the grafting of a functionalized PBA derivative to a functionalized platform polymer.^{14–16} Of particular note, PBA-functionalized hydrogel systems have been synthesized which exhibit reversible swelling responses to changes in the glucose concentration.^{10,17} Glucose binds to the tetrahedral ionized boronate species but does not form a stable bond with the trigonal uncharged boronic acid. As more glucose is added to the microgel environment, the driving force for PBA–glucose complexation increases and more boronate–glucose conjugates (Figure 1c) are generated. To maintain equilibrium at a given pH value, the boronic acid ionization equilibrium shifts to increase the concentration of the charged phenylboronate species (Figure 1b), effectively reducing the pK_a of the trigonal boronic acid functional groups. This equilibrium shift allows more glucose to bind to the PBA-functionalized polymer, which in turn triggers further PBA ionization until an equilibrium is reached at a given glucose concentration. As a result, when the PBA groups are anchored to a gel network, the anionic charge density within the gel increases as the glucose concentration is increased, driving a swelling response via both Donnan equilibrium and direct charge–charge repulsion effects. The PBA–

* To whom correspondence should be addressed: e-mail hoaretr@mcmaster.ca.

Table 1. Recipes Used To Prepare Microgels with the Same Bulk –COOH Content but Different –COOH Distributions

microgel	NIPAM (mol)	MBA (mol)	functional monomer (mol)	SDS (mol/L)	APS (mol/L)	–COOH content (mmol/g dry gel)
NIPAM	1.24×10^{-2}	6.5×10^{-4}	0	1.7×10^{-4}	4.4×10^{-4}	0.01 ± 0.02
AA–NIPAM	1.24×10^{-2}	6.5×10^{-4}	7.9×10^{-4}	1.7×10^{-4}	4.4×10^{-4}	0.53 ± 0.03
MAA–NIPAM	1.24×10^{-2}	6.5×10^{-4}	7.9×10^{-4}	1.7×10^{-4}	4.4×10^{-4}	0.52 ± 0.03
FA–NIPAM	1.24×10^{-2}	6.5×10^{-4}	6.9×10^{-4}	1.7×10^{-4}	4.4×10^{-4}	0.53 ± 0.03
VAA–NIPAM	1.24×10^{-2}	6.5×10^{-4}	34.9×10^{-4}	1.7×10^{-4}	4.4×10^{-4}	0.50 ± 0.02

glucose equilibrium similarly induces a feedback-controlled deswelling response as the glucose level decreases.

Glucose-responsive, PBA-functionalized hydrogel systems have a range of interesting potential applications. Bulk hydrogel-based glucose-sensing electrodes¹⁸ and colloidal crystalline arrays can detect physiological glucose concentrations according to the wavelength of diffracted light.¹⁵ Nucleotide separation, isolation, and sensing have been demonstrated using PBA-functionalized hydrogels,¹¹ microgels,⁶ porous polymeric beads,⁵ and linear polymers,¹⁴ often using poly(*N*-isopropylacrylamide) as the backbone polymer. The demonstrated mucoadhesivity of PBA-functionalized materials (i.e., their ability to selectively bind to the *cis*-diol-rich glycoproteins comprising mucous membranes) can facilitate site-specific drug delivery over a longer period of time than conventional delivery vehicles.¹⁹ Polymers with known protein-resistant properties (i.e., PEG) can similarly be modified with PBA to both covalently anchor the repellent polymers to tissue surfaces *in vivo* and prevent bioadhesion.¹⁶

However, despite the apparent swelling kinetics and fluid dynamics advantages of microgels in uptake/release and sensor applications, only limited attention has been devoted to the investigation of PBA-functionalized PNIPAM-based microgels in the literature. Elmas et al.⁶ produced NIPAM-*co*-VPBA microgels for nucleotide isolation and showed the effect of temperature on the colloidal stability and nucleotide adsorption/desorption capacity of the gels. However, the glucose-triggered swelling responses of the microgels were not investigated. Hazot et al.¹² synthesized *N*-ethylmethacrylamide-*co*-(phenylboronic acid methacrylamide) copolymer microgels and analyzed their copolymerization kinetics and thermal swelling behavior. The temperature response curves in this study were extremely broad, and glucose-induced swelling was not investigated. Zhang and Xu entrapped glucose oxidase in membrane-embedded methacrylic acid-functionalized PNIPAM microgels, facilitating glucose-mediated insulin release rates through the membrane pores.²⁰ However, the glucose oxidase in this case is only physically mixed with the microgels and thus would leach out over time in the physiological environment.

In response, we have devoted attention to the synthesis and optimization of PNIPAM-based PBA-functionalized microgels which possess well-defined glucose swelling or deswelling responses under a range of environmental conditions. In this work, the first in a series, we report on the synthesis and optimization of environmentally and colloidally stable microgels with glucose-responsive swelling capability. In particular, this paper describes how the functional group distributions of the microgels and the thermal phase transition can be engineered to produce novel tunable glucose swelling responses. The underlying functional group distribution is shown to strongly influence both the conjugation yield of PBA groups and the relative swelling responses of the different microgels upon glucose exposure. Furthermore, the multiresponsive nature of functionalized microgels is constructively applied to regulate glucose-induced swelling based on the simultaneous triggering of multiple types of phase transitions. This approach of using a

“secondary” phase transition (in this case, the thermal phase transition) to amplify or suppress a “primary” phase transition (in this case, the glucose-induced swelling) is a novel strategy to exploit the multiresponsive nature of these microgel systems to generate targeted glucose swelling responses, both overall and at specific glucose concentrations.

Experimental Section

Materials. *N*-Isopropylacrylamide (NIPAM, 99%, Acros Organics) was purified by recrystallization from a 60:40 toluene:hexane mixture. Methacrylic acid (MAA, 99%, Aldrich) and acrylic acid (AA, 99%, Aldrich) were purified by vacuum distillation. *N,N*-Methylenebis(acrylamide) (MBA, 99+%, Aldrich), vinylacetic acid (VAA, 97%, Aldrich), fumaric acid (FA, 99%, Aldrich), sodium dodecyl sulfate (SDS, 98%, Aldrich), ammonium persulfate (APS, 99%, BDH), *N*-3-dimethyl(aminopropyl)-*N'*-ethylcarbodiimide (EDC, commercial grade, Aldrich), and 3-aminophenylboronic acid (APBA, 98%, Aldrich) were all used as received. All water used in the synthesis and characterization was of Millipore Milli-Q grade.

Microgel Preparation. Polymerizations were conducted in a 250 mL three-necked flask fitted with a condenser and a glass stirring rod with a Teflon paddle. All monomers were dissolved in 150 mL of water and heated to 70 °C under a nitrogen purge. The initiator was then dissolved in 10 mL of water and injected into the preheated monomer mixture. Polymerization was allowed to proceed overnight (16 h), at which point the product microgel is cooled and purified by successive ultracentrifugation (170000g, 45 min) using a Beckman L55 ultracentrifuge. The product microgels are lyophilized and refrigerated for future use. Lyophilized and nonlyophilized samples of the same microgel were analyzed by light scattering to confirm that no significant differences are observed in glucose or thermal-induced swelling due to lyophilization.

Two series of microgels were evaluated. First, the well-defined carboxylic acid-functionalized microgels reported in our previous work^{21–23} were applied to investigate the effect of the functional group distributions in the graft platforms on the glucose responses of the PBA-graft microgels. The amount of methacrylic acid (MAA), acrylic acid (AA), fumaric acid (FA), and vinylacetic acid (VAA) used for each polymerization was determined such that the same total carboxylic acid content (6.5 mol % of the total monomer content) was achieved in each of the functionalized microgels (as confirmed by conductometric titration²¹). Synthetic recipes used to produce these bulk functionalization-matched microgels are shown in Table 1.

Second, a series of AA and VAA-functionalized microgels with different net –COOH concentrations were synthesized to investigate the impact of the degree of platform microgel functionalization on the APBA-graft microgel response. The recipes used in these preparations and the final carboxylic acid content of each of the microgels (as measured by conductometric titration) are given in Table 2. The microgels are labeled FM-NIPAM-*x*, where FM is the type of functional monomer used for the microgel preparation and *x* is the mole fraction of that functional monomer in the microgel (again, as measured via conductometric titration).

APBA Conjugation. Phenylboronic acid functional groups were incorporated into the microgel using EDC as a zero-length cross-linker to conjugate 3-aminophenylboronic acid (APBA) to the microgel-bound carboxylic acid groups. All conjugations were performed by suspending 36 mg of lyophilized microgel in 3.6 mL

Table 2. Recipes Used To Prepare Microgels with the Same –COOH Distribution but Different Bulk –COOH Contents

microgel	moles in feed					–COOH content (mmol/g gel)
	NIPAM	FM	SDS	MBA	APS	
AA–NIPAM-6.5	1.24×10^{-2}	7.9×10^{-4}	1.7×10^{-4}	6.5×10^{-4}	4.4×10^{-4}	0.53 ± 0.03
AA–NIPAM-11	1.24×10^{-2}	14×10^{-4}	1.7×10^{-4}	6.5×10^{-4}	4.4×10^{-4}	0.75 ± 0.03
AA–NIPAM-14	1.24×10^{-2}	17×10^{-4}	1.7×10^{-4}	6.5×10^{-4}	4.4×10^{-4}	1.05 ± 0.04
AA–NIPAM-22	1.24×10^{-2}	28×10^{-4}	2.7×10^{-4}	1.3×10^{-4}	4.4×10^{-4}	1.34 ± 0.03
VAA–NIPAM-6.5	1.24×10^{-2}	35×10^{-4}	1.7×10^{-4}	6.5×10^{-4}	4.4×10^{-4}	0.50 ± 0.02
VAA–NIPAM-8.0	1.24×10^{-2}	47×10^{-4}	1.7×10^{-4}	6.5×10^{-4}	4.4×10^{-4}	0.65 ± 0.03

of MES buffer (pH 4.8, 20 mM ionic strength). APBA solutions were prepared at different concentrations ranging from 1 up to 10 mg/mL in the same 20 mM, pH 4.8 MES buffer. A volume of 3.6 mL of the desired APBA solution was added to the microgel suspension and mixed under gentle magnetic stirring at 15 °C. After ~30 min, 1.0 mL of a freshly prepared EDC solution varying in concentration between 5 and 50 mg/mL was added to the vials. Each conjugation reaction was allowed to proceed for 2 h, at which point the microgel conjugates are immediately ultracentrifuged four times to remove unreacted APBA and EDC as well as the soluble urea byproduct of EDC cross-linking. All of the product microgel conjugates are assigned the code *Ap Eq*, where *p* is the concentration of the APBA solution and *q* is the concentration of EDC solution mixed together to perform the conjugation (both in mg/mL). For example, to prepare the microgel APBA-AA-6.5 A5 E50, 3.6 mL of a 5 mg/mL APBA solution and 1.0 mL of a 50 mg/mL EDC solution were added to 3.6 mL of a 10 mg/mL AA-NIPAM-6.5 microgel suspension. All APBA and EDC concentrations used were in at least 2-fold molar excess to the total number of –COOH groups present in the microgels used in this study. The microgels were stored in suspension at 4 °C.

Microgel Characterization. ¹H NMR analysis was conducted using a Bruker 600 MHz spectrometer. Lyophilized microgels were suspended in D₂O (Cambridge Isotope Laboratories) to acquire the spectra at room temperature (i.e., the fully swollen state). Phenylboronic acid contents of the PBA–microgel conjugates were measured on the basis of the integrated intensity ratio of the aromatic hydrogen peaks (δ 7.2–7.6 ppm) and the –CH group peak from NIPAM (δ 3.9 ppm). Long relaxation times were used to ensure optimal relaxation of the gel network prior to the application of a subsequent pulse. Particle sizing was performed by dynamic light scattering using a detector angle of 90°. A Lexel 95 ion laser operating at a wavelength of 514 nm and a power of 100 mW was used as the light source. Correlation data were analyzed using a BI-9000AT digital autocorrelator, version 6.1 (Brookhaven Instruments Corp.). At least five replicates were conducted for each sample; the experimental uncertainties represent the standard deviation of the replicate measurements. Electrophoretic mobility values were measured using a ZetaPlus analyzer (Brookhaven Instruments Corp.) operating in phase analysis light scattering (PALS) mode. A total of 10 runs (each comprised of 15 cycles) were conducted; the experimental uncertainties represent the standard error of the mean of the replicate runs. Samples were typically prepared in thoroughly cleaned vials by suspending a small quantity of lyophilized microgel in 0.005 M pH 9 carbonate buffer. Glucose was added to selected samples in physiologically relevant concentrations. Physiological blood glucose levels of interest are within the range 0–3 g/L,¹⁸ with 0.9–1.30 g/L (5.0–7.2 mM) being the “normal” range.²⁴

Results and Discussion

The effects of the underlying functional group distribution and the total functional group content of the platform microgels on the glucose responsiveness of PBA-graft microgels were both analyzed and will be considered separately in the following discussion.

Effects of Functional Group Distributions. In our previous work, the radial and chain functional group distributions of microgels functionalized with MAA, AA, VAA, and FA were









identified, via both experimental analysis^{21,23} and copolymerization kinetics modeling.²² Using the “graft-to” PBA incorporation technique, these well-defined microgels can be applied as conjugation platforms for the PBA grafting reaction, providing a facile method for controlling the distribution of PBA functional groups inside the microgel.

Effect of Functional Group Distributions on PBA Conjugation Yield. As Table 3 indicates, both the chain and radial functional group distributions influence the efficiency of PBA conjugation to microgels. APBA and EDC were added in 10-fold and 100-fold molar excesses, respectively, compared to the total number of –COOH groups present to ensure maximum overall conjugation yields are achieved in each of the microgels. The covalent nature of the microgel–APBA conjugation was also confirmed using a control sample in which the APBA solution and microgel suspension were mixed, but no EDC was added. As shown in Table 3, no APBA was detected in this microgel after purification, and no significant change was observed in either the particle size or electrophoretic mobility after PBA conjugation. Thus, the APBA present in the EDC-treated microgels is covalently attached to the microgels.

The relative conjugation yields in the different microgels can be correlated with the radial and chain functional group distributions in those microgels, which are illustrated schematically in Table 3. In general, the conjugation efficiency increases as the functional group distribution in the platform microgel becomes more radially surface localized and chain delocalized. These effects can be rationalized on the basis of both steric and diffusive factors. Covalent conjugation can only occur when both the APBA ligand and the EDC cross-linker diffuse sufficiently close to a –COOH group in the platform microgel network to react. Localizing functional groups near the more lightly cross-linked microgel surface reduces the need for APBA and EDC diffusion through the microgel matrix during conjugation. Concurrently, maximizing the distance between functional residues along the polymer chains reduces steric crowding limiting the grafting of two PBA groups to adjacent functional sites.

VAA–NIPAM has both a highly surface-localized radial –COOH distribution and a well-isolated chain –COOH distribution.²⁵ Consequently, the conjugation reactions can proceed unhindered by steric or diffusive barriers, allowing for an extremely high conjugation efficiency to be achieved. Conjugation efficiencies this high (~95%) have not previously been reported in the microgel literature, demonstrating the benefits of the unique, chain-end-functionalized morphology of VAA–NIPAM attributable to the chain transfer mechanism of VAA incorporation.²⁵ Furthermore, the acrylamide-based PBA monomers typically used to prepare PBA–hydrogel conjugates (i.e., acrylamino-phenylboronic acid or methacrylamino-phenylboronic acid) are both somewhat faster reacting and more hydrophobic than NIPAM, promoting their incorporation within the bulk of the microgel as opposed to the surface. Thus, the VAA–NIPAM graft platform approach to synthesizing PBA–microgels has a

Table 3. PBA Content and Conjugation Efficiency Resulting from APBA Conjugation Reactions^a

Microgel	Radial Functional Group Distribution	Chain Functional Group Distribution	ABPA:NIPAM Molar Ratio (%)	Conjugation Efficiency (%)
MAA-NIPAM			3	46.2
AA-NIPAM			4.5	69.2
VAA-NIPAM			6.2	95.4
FA-NIPAM			4.8	73.4
AA-NIPAM, no EDC	N/A	N/A	0.1	1.5

^a The APBA:NIPAM molar ratio is measured via ¹H NMR while the conjugation efficiency is the percentage of the total number of -COOH groups in the microgel which react with APBA during the conjugation reaction. radial functional group distributions are calculated as per ref 22; darker shadings represent higher local -COOH densities. Chain functional group distributions are schematic representations of the titration results from ref 21.

distinct advantage in terms of facilitating high yields of highly surface-localized PBA functional groups.

Although FA-NIPAM also has a highly surface-localized radial -COOH distribution, the diacid nature of the monomer provides significant steric inhibition to the conjugation of a second APBA molecule at the same FA monomer residue.²¹ As a result, the conjugation efficiency of APBA to FA-NIPAM is significantly lower than that observed for VAA-NIPAM despite the similar apparent radial functional group distributions in the two microgels. The degree of conjugation achieved with AA-NIPAM, which has a near-uniform radial functional group distribution and a relatively isolated chain -COOH distribution,²¹ is very similar to that achieved with FA-NIPAM. In this case, the negative effect of the more bulk-functionalized radial functional group distribution (i.e., a diffusive disadvantage) is offset by the higher average separation of the -COOH groups within the polymer chains (i.e., a steric advantage). Finally, MAA-NIPAM contains a significant number of functional monomer blocks and a core-localized radial distribution of -COOH groups.²¹ Correspondingly, both steric and diffusive barriers exist to PBA conjugation, and MAA-NIPAM exhibited the lowest degree of conjugation.

Effect of Functional Group Distributions on Glucose-Induced Swelling. The glucose responsiveness of the different conjugate microgels is also highly dependent on the underlying functional group distribution of the platform microgel. Figure 2 presents the observed changes in particle size (Figure 2a) and light scattering intensity (Figure 2b) of the PBA-microgel conjugates in response to changes in the glucose concentration. It should be noted that borate buffer (5 mM, pH 9) experiments were also performed to confirm that the microgel swelling responses observed in Figure 2 were induced by specific PBA-

glucose interactions. Free borate competitively binds glucose, reducing the amount of glucose bound to the microgel and thus the swelling response observed. When APBA-VAA-8.0 is exposed to 1 mg/mL glucose, a 28% increase in volume is observed in borate buffer while a 90% increase in volume is observed in carbonate buffer at the same ionic strength. Given this demonstrated borate ion interference, the changes in microgel size shown in Figure 2 must be related to specific PBA-glucose binding.

With the exception of the EDC-free control, each microgel displays a swelling response to even the smallest physiologically relevant glucose concentration. This swelling response is a direct result of the equilibrium shown in Figure 1 and described in the Introduction. As the glucose concentration increases, more anionic boronate species are generated, and the net anionic charge density of the microgel increases. The general trend in the particle swelling data correlates with the underlying functional group distribution in the platform microgel. As microgel-bound -COOH groups in the platform microgel (and thus the PBA groups in the graft microgel) become more surface-localized and chain-delocalized, higher magnitude swelling responses are achieved upon glucose binding. This response is directly in parallel with that observed in the pH-induced swelling of the different microgels,²¹ reasonable given that both the pH- and glucose-driven phase transitions in microgels are induced by changes in the net ionic charge of the microgel. Again, this observation confirms the advantage of using a graft-to approach for PBA conjugation as opposed to a copolymerization approach in which the majority of PBA groups are not incorporated at or near the microgel surface. The actual quantity of PBA conjugated to each of these microgels (as per Table 3) also influences the degree of glucose-responsive swelling

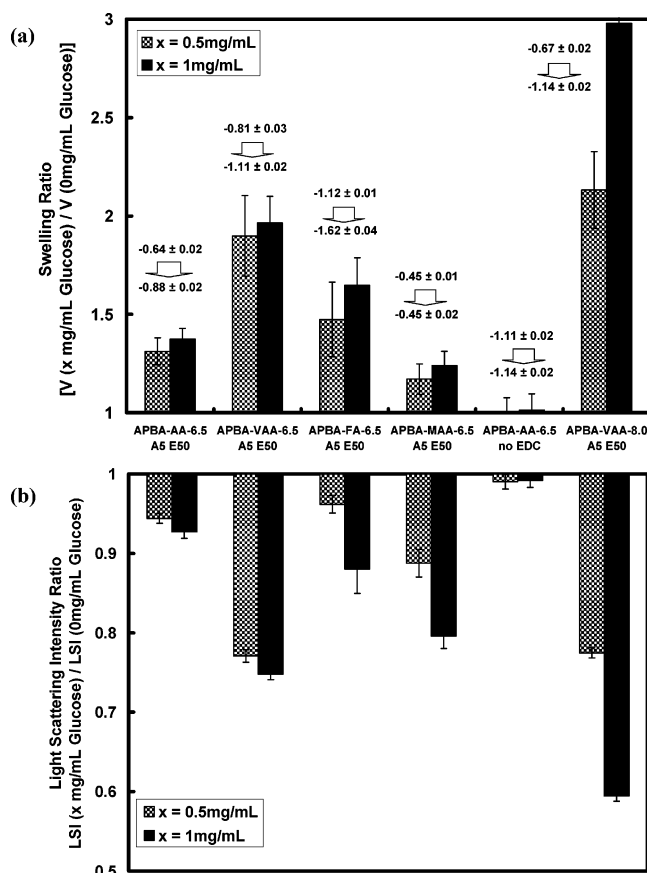


Figure 2. Ratio change in hydrodynamic volume, V (a), and light scattering intensity, LSI (b), as a function of glucose concentration for the APBA-modified microgels at pH 9 and 25 °C (5 mM ionic strength). The y-axis in both cases represents the ratio between the hydrodynamic diameter or light scattering intensity in an x mg/mL glucose solution (where $x = 0.5$ or 1 mg/mL) and the same variable in a glucose-free solution. The corresponding electrophoretic mobilities in the presence of 0 mg/mL (top) and 1 mg/mL (bottom) glucose are also shown in panel (a).

observed; microgels containing higher PBA contents (VAA–NIPAM) swell more than microgels with lower PBA contents (MAA–NIPAM).

In general, the light scattering and particle size data show parallel responses: the larger the macroscopic swelling achieved upon glucose addition, the larger the observed decrease in the light scattering intensity of the microgel. However, the relative magnitudes of these responses are significantly different according to the radial functional group distributions in the microgels. Although APBA–MAA-6.5 contains the lowest bound fraction of PBA (46% PBA incorporation, Table 3) and swells less than half as much as APBA–FA-6.5 upon ionization (Figure 2a), the reduction in light scattering intensity upon the addition of 1 mg/mL glucose in APBA–MAA-6.5 is more than double that observed for APBA–FA-6.5 (Figure 2b). This is a direct result of the presence of the APBA grafts in the more densely cross-linked core of APBA–MAA-6.5. In this case, glucose binding induces ionization and thus swelling in the densest region of the microgel, which scatters the most light. Thus, even the relatively small degree of swelling shown in Figure 2a results in a relatively large change in the light scattering intensity. Conversely, the larger number of APBA residues grafted within the more lightly cross-linked, near-surface region of APBA–FA-6.5 results in a large increase in the particle diameter but a relatively small decrease in the light scattering intensity given that the denser microgel core remains unswollen.

Table 4. Ratio Changes in Hydrodynamic Volume and Light Scattering Intensity in the Presence of 1 mg/mL Glucose at Different Temperatures (pH 9, 5 mM Carbonate Buffer)

microgel	ratio (x (1 mg/mL glucose)/ x (0 mg/mL glucose))	
	x = hydrodynamic volume	x = light scattering intensity
APBA–AA-22 A2 E10	1.28 ± 0.09	0.31 ± 0.01
APBA–AA-22 A2 E20	1.54 ± 0.07	0.19 ± 0.01
APBA–AA-22 A5 E20	3.54 ± 0.17	0.15 ± 0.01
APBA–AA-22 A5 E100	28.5 ± 0.20	0.06 ± 0.01

This latter observation has a practical impact on the application of these microgels as glucose sensors. Microgel performance in a swelling-based sensor application would be optimized using a surface-functionalized graft platform to facilitate the largest swelling response in the presence of glucose. In comparison, the performance of a turbidimetric glucose sensor may be optimized using a core-functionalized graft platform to facilitate the largest light scattering intensity response to a given increase in glucose concentration.

The glucose responses of the microgels can be regulated by changing both the glucose concentration and the $-\text{COOH}$ content of the microgel. As evidence for the former claim, each microgel swells more and scatters less light in 1.0 mg/mL glucose solutions compared to 0.5 mg/mL glucose solutions, although the volume ratio error bars do in some cases overlap. Thus, regardless of the morphology, systematic and concentration-dependent responses can be achieved to changes in the external glucose concentration. To illustrate the latter claim, a VAA–NIPAM microgel with 8 mol % VAA was synthesized and subjected to the same PBA conjugation conditions as the other microgels. As anticipated, more APBA was conjugated to the microgel (7.1% APBA:NIPAM ratio according to ^1H NMR compared to 6.2% for APBA–VAA-6.5), and correspondingly larger glucose-triggered responses were observed in both the particle size (Figure 2a) and the light scattering intensity (Figure 2b). Thus, in general, the $-\text{COOH}$ content of the microgel graft platform determines the magnitude of the glucose swelling response of the conjugate while the choice of comonomer determines the relative responses of the light scattering intensity and particle size to glucose concentration fluctuations.

Effects of Functional Group Content. The VAA–NIPAM result in Figure 2 suggests that the bulk content of reactive $-\text{COOH}$ residues in the platform microgel has a significant impact on the magnitude of the glucose-induced swelling observed in PBA-functionalized microgels. Indeed, both the $-\text{COOH}$ concentration in the platform microgel and the PBA concentration in the graft conjugate can be used to tune the glucose-driven swelling response within specific temperature and/or glucose concentration ranges.

Swelling Enhancement by Gel Compositional Changes. In any functionalized microgel, the swelling response to a specific stimulus can be maximized by increasing the concentration of the environmentally responsive functional groups (increasing the specific driving force for swelling) and/or decreasing the cross-link density (reducing the elastic resistance to swelling). Table 4 shows the volumetric swelling and light scattering responses for a 22 mol % acrylic acid-functionalized microgel containing 1 mol % cross-linker and different PBA contents. In comparison, the AA-functionalized microgel used as the grafting platform to synthesize the APBA–AA–NIPAM microgel in Figure 2 contains 6.5 mol % acrylic acid and 4.5 mol % cross-linker. Up to 30-fold increases in volume and 95%

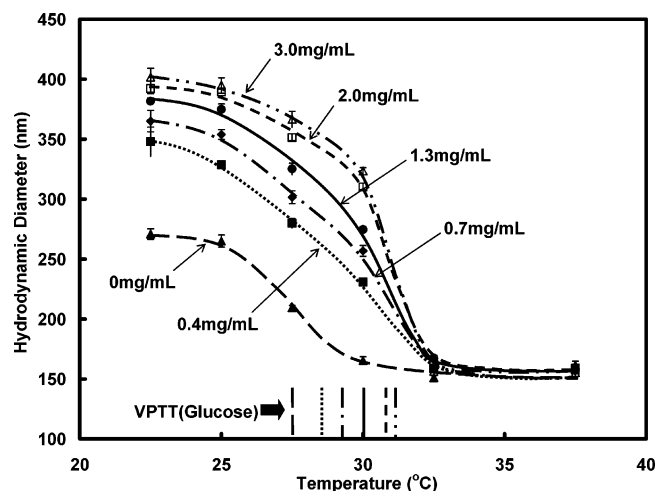


Figure 3. Hydrodynamic diameter vs temperature profiles for the APBA-AA-11 A5 E50 microgel in the presence of physiologically relevant glucose concentrations at pH 9. The hash marks along the x-axis illustrate the systematic changes in the midpoint VPTT value of the microgel at each plotted glucose concentration.

decreases in light scattering intensity can be achieved in the presence of just 1 mg/mL glucose when microgels with high $-\text{COOH}$ contents (i.e., more PBA binding sites) and lower cross-link densities are used as the conjugation platforms. The volume and light scattering changes scale with the PBA content of the microgel: the higher the APBA and EDC concentrations used to prepare the conjugates, the more PBA is incorporated into the microgel and larger the light scattering and hydrodynamic diameter changes are observed upon glucose exposure.

Swelling Response Enhancement by Phase Transition Amplification. Alternately, the multiresponsive nature of PNIPAM-based PBA-functionalized microgels can be applied to amplify a targeted phase transition by controlling a secondary variable. Of particular interest, the glucose-induced swelling response of a microgel can be either amplified or suppressed by tuning the absolute temperature and magnitude of the LCST shift observed upon glucose binding. Figure 3 illustrates that a systematic, glucose-induced VPTT shift occurs in PBA-microgel conjugates. A $\sim 4^\circ\text{C}$ VPTT shift is observed for the APBA-AA-11 A5 E50 microgel as the glucose concentration increases from 0 to 3 mg/mL, with the VPTT increasing systematically as the glucose concentration increases. This VPTT shift has a significant influence on the glucose swelling response of the microgel, as indicated schematically in Figure 4. At 15°C ($T \ll \text{VPTT}$), all of the observed $\sim 30\%$ increase in microgel particle size upon exposure to 1 mg/mL glucose can be attributed to the PBA ionization equilibrium swelling mechanism (Figure 1). This swelling measurement can therefore be used as a baseline value to evaluate the effect of the thermal phase transition on the glucose swelling response at higher temperatures. At $T > 35^\circ\text{C}$, no glucose sensitivity whatsoever is observed in the microgel, suggesting that the thermal transition can effectively suppress the PBA ionization-driven microgel swelling at $T > \text{VPTT}$. Mechanistically, this observation indicates that the hydrophobic interactions driving thermal gel collapse can overwhelm the ionization driving force of glucose-induced swelling. Conversely, within the volume phase transition temperature range $25^\circ\text{C} < T < 32^\circ\text{C}$ (i.e., between the onset VPTT in the absence of glucose and the offset VPTT in the presence of glucose), PBA ionization-driven swelling is amplified by the thermal swelling resulting from the VPTT shift upon glucose binding. Using the $T = 30^\circ\text{C}$ data as an example, the microgel is fully collapsed in the absence of glucose (VPTT \sim

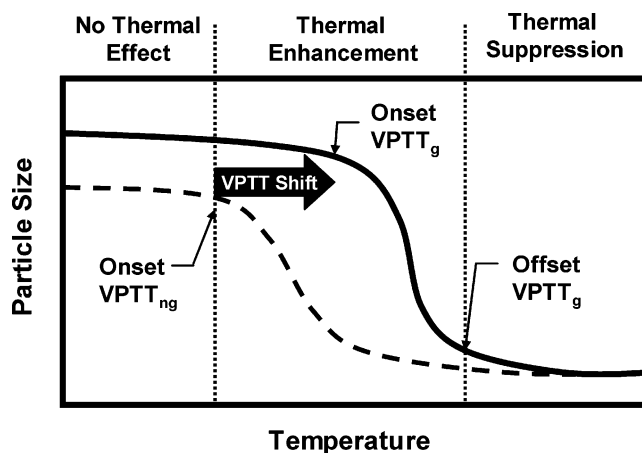


Figure 4. Schematic diagram of the effect of the thermal volume phase transition on the glucose swelling response of a PBA-functionalized microgel as a function of temperature. Microgel phase transition temperatures are indicated as VPTT_{ng} (no glucose present) and VPTT_{g} (glucose present).

$27^\circ\text{C} < T$) but is significantly swollen in the presence of 2 mg/mL glucose (VPTT $\sim 31^\circ\text{C} > T$). As a result, if the microgel device is operated at 30°C , an 8-fold volume increase is observed as the glucose concentration increases from 0 to 2 mg/mL, a significantly larger response than the baseline 3-fold volume change observed at 15°C . Identical trends are observed in the corresponding light scattering intensity profiles.

These results suggest that the VPTT shift observed as the glucose concentration increases permits highly sensitive switching of microgel swelling according to the temperature or glucose concentration. At a fixed glucose concentration, increasing the temperature by $\sim 5^\circ\text{C}$ can switch the swelling from being thermally amplified at 30°C to being thermally suppressed at 35°C , enabling the use of this microgel as a sensitive “on–off” switch. Conversely, at a fixed temperature, the microgel can be tuned to achieve enhanced swelling and/or light scattering intensity responses over specific glucose concentration ranges. Figure 5 shows how the temperature can strongly affect not only the magnitude but also the trajectory of the volume and scattering intensity responses to glucose concentration. Glucose concentrations are chosen to represent physiologically relevant situations; 0.4 g/L is the hypoglycemic limit, 0.7–1.3 g/L is the normal glucose concentration in blood, and 2 g/L is the hyperglycemic limit.

At 25°C , the onset VPTT of the microgel in the absence of glucose lies below the test temperature while the VPTT at any of the tested glucose concentrations lies above the test temperature. Consequently, a large swelling response is observed when even a small amount of glucose is added due to thermal phase transition amplification; higher glucose concentrations correspondingly have virtually no impact on gel swelling. In contrast, at 27.5°C , the microgel VPTT values at glucose concentrations < 1.3 g/L also lie below the test temperature. As a result, a large, thermally assisted swelling event is observed as the glucose concentration increases from 1.3 to 2 g/L (interestingly, the concentration range over which insulin release would be desirable to avoid hyperglycemia). A similar trend is observed using 30°C as the test temperature, particularly in the light scattering intensity profile (Figure 5b). When the temperature is just above (32.5°C) or just below (22.5°C) the VPTT range, the microgel is only minimally responsive to changes in the glucose concentration, with the swelling response effectively “turned off” at $T > \text{VPTT}$. Thus, by changing the temperature at which a PBA-microgel conjugate is used,

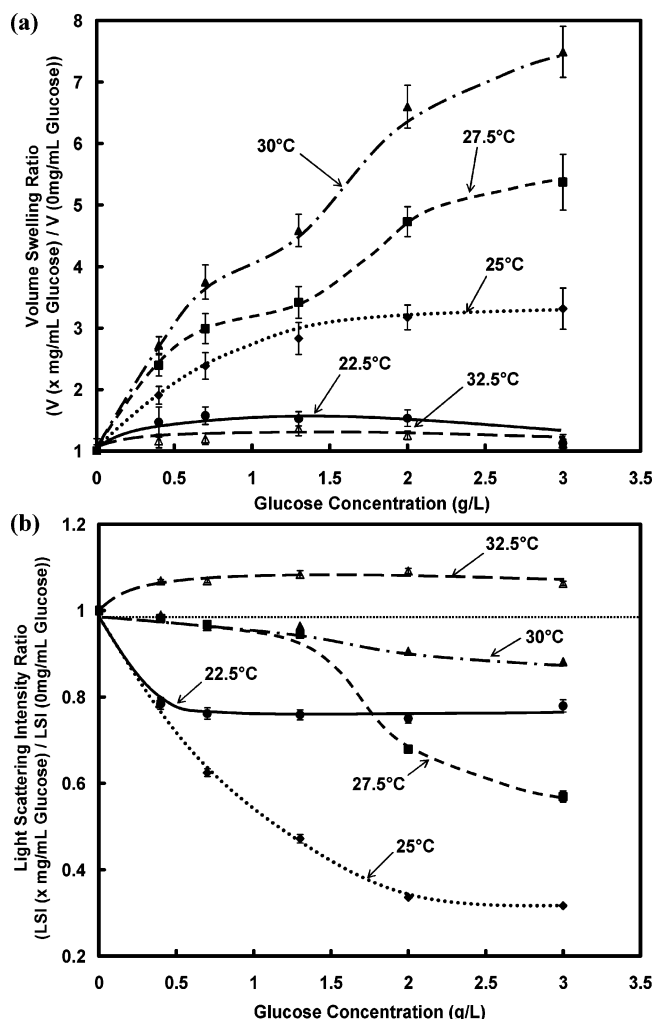


Figure 5. Volumetric (a) and light scattering intensity (b) responses for APBA-AA-11 A5 E50 as a function of glucose concentration as measured at different test temperatures (pH 9, 5 mM carbonate buffer).

different glucose response profiles can be achieved to provide more or less resolution to changes in the external glucose concentration within specific, tunable glucose concentration ranges.

Tuning Thermal Enhancement of the Glucose Phase Transition. The temperature and glucose concentration range over which the glucose-induced phase transition is thermally enhanced can be controlled by several factors. Table 5 shows how the density of PBA grafts to a specific platform microgel can regulate the swelling response. The VPTT of the unmodified 11 mol % AA-NIPAM microgel platform is $\sim 60^\circ\text{C}$, well above both test temperatures. As more APBA or EDC is added to the conjugation mixture, more APBA is grafted to the microgel, increasing the microgel hydrophobicity and reducing the VPTT. At 25°C , the VPTT of each of the APBA-modified microgels lies above the test temperature, resulting in a systematic increase in glucose-induced gel swelling as more APBA is incorporated into the microgels. A similar trend exists at 37°C for the two microgels with the lowest APBA content. However, the PBA contents of both the A5 E10 and A5 E20 microgels are sufficiently high such that the VPTT of each of these microgels lies close to (A5 E10) or below (A5 E20) the 37°C test temperature. As a result, the glucose response is restricted in the A5 E10 microgel and effectively “shut off” in the A5 E20 microgel by the thermal phase transition. This observation suggests that the temperatures at which both thermal amplification and suppression of the glucose-triggered phase

transition occurs can be tuned according to the PBA content of the conjugate. Thus, the incorporation of more PBA functional groups into the microgel may not result in higher degrees of microgel swelling depending on the test temperature of the microgel device.

Similar control over the VPTT can be exercised by adjusting the number of unreacted carboxylic acid functional groups in the microgel. As the number of residual $-\text{COOH}$ groups in the microgel increases, the VPTT of the base microgel also increases. Thus, by increasing the carboxylic acid content of the platform microgel, conjugates can be prepared which contain the same number of PBA groups (and thus show the same ionization-driven glucose response) but exhibit thermally enhanced glucose swelling at higher temperatures. Indeed, Table 5 indicates that glucose-induced swelling of the APBA-AA-11 A5 E20 microgel is suppressed by the thermal transition at 37°C while the corresponding APBA-AA-22 A5 E20 microgel swells more than 3-fold by volume under the same conditions owing to its higher residual $-\text{COOH}$ concentration (and thus higher VPTT).

Sensor Implications. The demonstrated tunability of the PBA-microgel swelling according to the total $-\text{COOH}$ and PBA content in the platform microgel is particularly beneficial in the design of sensors with linear glucose concentration responses over targeted glucose concentration ranges. Figure 6 shows that linear diameter and light scattering intensity responses can be achieved over different glucose concentration ranges by tuning the underlying $-\text{COOH}$ content of the platform microgel to control the PBA content of the microgel. As the PBA content of the microgel increases, the magnitude of the overall glucose response increases and the glucose concentration range over which linear particle size and light scattering intensity responses are observed narrows. These trends can both be rationalized according to the PBA equilibrium shown in Figure 1. As the number of PBA groups present in the microgel matrix increases, a smaller change in the glucose concentration can drive larger increases in the gel phase degree of ionization due to the higher number of responsive functional groups present in the gel matrix. Furthermore, at higher degrees of PBA functionalization, the average spacing between an ionized boronate group and an adjacent nonionized boric acid residue decreases such that the inductive reduction in the effective boric acid pK_a becomes more efficient in driving the equilibrium shift shown in Figure 1 at lower glucose concentrations. This accounts for the steeper slope of the curves as the PBA fraction in the microgels increases. Thus, the number and distribution of PBA groups in the microgel can be used to design glucose sensors with large responses over specific glucose concentration ranges.

The functional monomer used to prepare the base microgel can also be used to tune the nature of the glucose-induced swelling, as shown in Figure 7. The effect of functional group distributions on glucose-induced microgel swelling can be illustrated by comparing the deswelling profiles of the APBA-AA-6.5 and APBA-FA-6.5 microgels, both of which have approximately the same PBA and residual $-\text{COOH}$ content according to the ^1H NMR results. Both microgels swell ~ 2 -fold by volume when exposed to 1 mg/mL glucose at 15°C . However, APBA-AA-6.5 shows a clear VPTT shift, facilitating a thermally enhanced 5-fold volumetric swelling upon exposure to 1 mg/mL glucose at 27.5°C , and maintains at least some glucose swelling activity at temperatures as high as 35°C . Conversely, APBA-FA-6.5 exhibits no significant VPTT shift, swells no more than 2-fold by volume in the presence of 1 mg/mL glucose at any temperature, and loses all glucose activity

Table 5. Ratio Changes in Hydrodynamic Volume and Light Scattering Intensity (LSI) in the Presence of 1 mg/mL Glucose at Different Temperatures (pH 9, 5 mM Carbonate Buffer)

microgel	ratio $[x(1 \text{ mg/mL glucose})/x(0 \text{ mg/mL glucose})]$			
	$T = 25^\circ\text{C}$		$T = 37^\circ\text{C}$	
	$x = \text{volume}$	$x = \text{LSI}$	$x = \text{volume}$	$x = \text{LSI}$
APBA-AA-11 A1 E5	1.26 ± 0.15	0.81 ± 0.01	1.37 ± 0.09	0.82 ± 0.01
APBA-AA-11 A1 E10	1.60 ± 0.12	0.69 ± 0.01	4.25 ± 0.30	0.84 ± 0.01
APBA-AA-11 A5 E10	3.11 ± 0.27	0.65 ± 0.01	3.72 ± 0.21	0.90 ± 0.02
APBA-AA-11 A5 E20	7.65 ± 0.33	0.56 ± 0.01	1.26 ± 0.13	1.05 ± 0.03

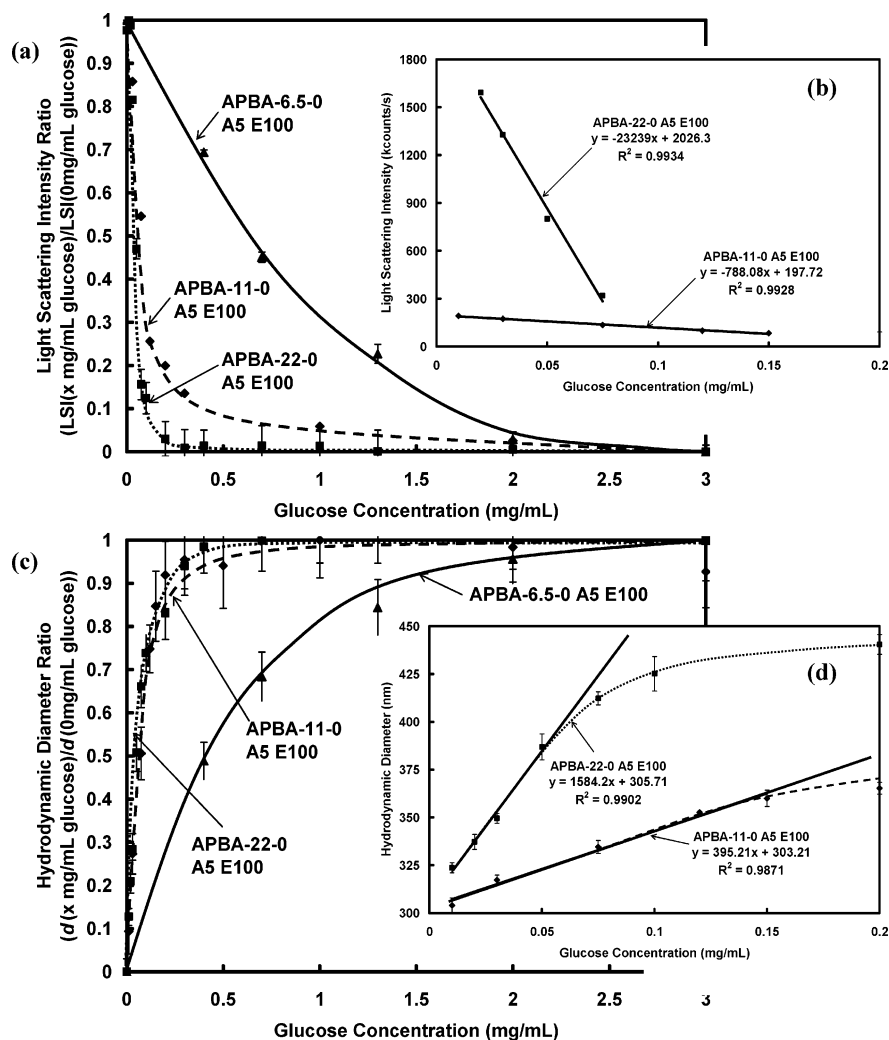


Figure 6. Hydrodynamic diameter and light scattering responses of a series of microgels with different total PBA contents (pH 9, 25 °C, 5 mM ionic strength): (a) light scattering intensity ratio (relative to zero-glucose); (b) light scattering intensity trend expanded for the APBA-22-0 and APBA-11-0 microgels in the 0–0.2 mg/mL glucose range; (c) hydrodynamic diameter ratio (relative to zero glucose); (d) hydrodynamic diameter trend expanded for the APBA-22-0 and APBA-11-0 microgels in the 0–0.2 mg/mL glucose range.

at $T > 30^\circ\text{C}$. VAA–NIPAM-6.5 exhibits even larger thermal enhancements than observed for the APBA–AA-6.5 microgels.

Interestingly, at high temperatures, the particle size of APBA–FA-6.5 in the presence of 1 mg/mL glucose is lower than that of the same gel in the absence of glucose. This suggests that the highly surface-localized and (in some cases) paired PBA groups in APBA–FA-6.5 facilitate the formation of cross-links between two polymer-supported PBA groups and glucose. Glucose contains two *cis*-diol binding sites and can bridge two PBA groups to form (reversible) covalent cross-links in dense gel networks.¹⁵ Thus, although the charge density in the microgel increases upon glucose binding, the concurrent increase in the cross-link density accounts for the reduced degree of swelling (or, at higher temperatures, deswelling) via elastic constraints. In contrast, the functional groups are radially delocalized within

the APBA–AA-6.5 microgel and extremely chain-delocalized in the APBA–VAA-6.5 microgel such that cross-linking is less probable and the particle size increases at all temperatures upon glucose addition. This cross-linking mechanism also explains the lack of a significant glucose-induced VPTT shift in APBA–FA-6.5 despite the large VPTT shifts observed in the other microgels.

Overall, the VPTT of PBA–microgel conjugates can be tuned to amplify or suppress the glucose-induced phase transition within specific glucose concentration and temperature ranges by controlling the content and distribution of graft sites in the platform microgel (via the polymerization recipe) or the degree of APBA conjugation in the graft microgel (via the EDC/APBA concentrations used for the conjugation). In addition, several different temperature switches can easily be prepared from the

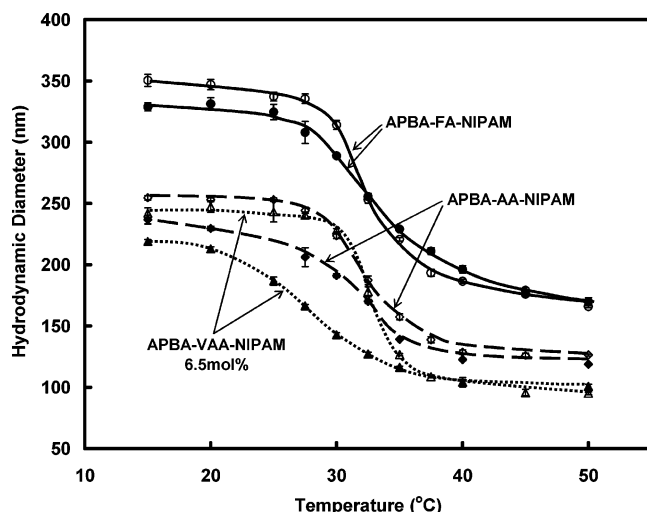


Figure 7. Hydrodynamic diameter vs temperature profiles for PBA-microgel conjugates prepared using microgel platforms with different functional group distributions (pH 9, 5 mM carbonate buffer). The filled points represent the size profile in the absence of glucose while the unfilled points show the diameters in the presence of 1 mg/mL glucose.

same platform microgel using different conjugation conditions in the graft-to approach described, facilitating the synthesis of multitemperature responsive microgel mixtures if desired. However, it must be noted that these microgels exhibit only minimal glucose responsiveness at pH 7.4. Future papers in this series will describe how the general design principles developed in this work (i.e., using the thermal phase transition to enhance glucose swelling and engineering the functional group distributions in the platform microgels) can be applied to produce microgels which deswell in response to glucose exposure and microgels which exhibit on-off glucose swelling responses under physiological pH, temperature, and ionic strength conditions.

Conclusions

(1) Phenylboronic acid-modified poly(*N*-isopropylacrylamide)-based microgels exhibit reversible swelling responses to changes in the environmental glucose concentration.

(2) Conjugation of aminophenylboronic acid to -COOH-functionalized microgels is enhanced as reactive functional groups in the platform microgels are localized on the microgel surface and randomly distributed within the polymer subchains of the gel network.

(3) The functional group distributions in the platform microgel control the relative changes in the turbidity and particle volume as the glucose concentration is increased while the total number of PBA groups present in the microgel controls the absolute magnitude of glucose-induced swelling.

(4) The thermal phase transition can be applied to either amplify or suppress the PBA ionization-driven glucose swelling phase transition, providing highly selective control over the

glucose swelling response of a particular PBA-graft microgel particle. Up to 4-fold amplifications in volumetric swelling responses can be achieved by tuning the VPTT of the microgel conjugates.

(5) Both the temperature ranges and the glucose concentration ranges over which glucose swelling amplification and suppression are achieved can be tuned by changing the underlying composition of the platform microgel and/or the amount of PBA grafted to the microgels. Linear glucose concentration sensors can therefore be designed with specific sensitivities to targeted glucose concentration ranges.

Acknowledgment. The Natural Sciences and Engineering Research Council of Canada (NSERC) is acknowledged for funding this work.

References and Notes

- (1) Kost, J.; Horbett, T. A.; Ratner, B. D.; Singh, M. *J. Biomed. Mater. Res.* **1985**, *19*, 1117–1133.
- (2) (a) Kokufuta, E.; Zhang, Y. Q.; Tanaka, T. *Nature (London)* **1991**, *351*, 302–304. (b) Brownlee, M.; Cerami, A. *Science* **1979**, *206*, 1190–1191. (c) Seminoff, L. A.; Olsen, G. B.; Kim, S. W. *Int. J. Pharm.* **1989**, *54*, 241–249.
- (3) Vignon, L. *C. R. Acad. Sci.* **1874**, *78*, 148–149.
- (4) Böeseken, J. *Carbohydr. Chem.* **1947**, *4*, 189–210.
- (5) Senel, S.; Camli, S. T.; Tuncel, M.; Tuncel, A. *J. Chromatogr. B* **2002**, *769*, 283–295.
- (6) Elmas, B.; Onur, M. A.; Senel, S.; Tuncel, A. *Colloids Surf., A* **2004**, *232*, 253–259.
- (7) Kataoka, K.; Miyazaki, H.; Okano, T.; Sakurai, Y. *Macromolecules* **1994**, *27*, 1061–1062.
- (8) Shimori, K.; Ivanov, A. E.; Galaev, I. Y.; Kawano, Y.; Mattiasson, B. *Macromol. Chem. Phys.* **2004**, *205*, 27–34.
- (9) Kitano, S.; Kataoka, K.; Koyama, Y.; Okano, T.; Sakurai, Y. *Makromol. Chem., Rapid Commun.* **1991**, *12*, 227–233.
- (10) Matsumoto, A.; Kurata, T.; Shiino, D.; Kataoka, K. *Macromolecules* **2004**, *37*, 1502–1510.
- (11) Kanekiyo, Y.; Sano, M.; Iguchi, R.; Shinkai, S. *J. Polym. Sci., Part A* **2000**, *38*, 1302–1310.
- (12) Hazot, P.; Delair, T.; Elaïssari, A.; Chapel, J.-P.; Pichot, C. *Colloid Polym. Sci.* **2002**, *280*, 637–646.
- (13) De Geest, B. G.; Jonas, A. M.; Demeester, J.; De Smedt, S. C. *Langmuir* **2006**, *22*, 5070–5074.
- (14) Uguzdogan, E.; Kayi, H.; Denkbaz, E. B.; Patir, S.; Tuncel, A. *Polym. Int.* **2003**, *52*, 649–657.
- (15) Alexeev, V. L.; Sharma, A. C.; Goponenko, A. V.; Das, S.; Lednev, I. K.; Wilcox, C. S.; Finegold, D. N.; Asher, S. A. *Anal. Chem.* **2003**, *75*, 2316–2323.
- (16) Winblade, N. D.; Nikolic, I. D.; Hoffman, A. S.; Hubbell, J. A. *Biomacromolecules* **2000**, *1*, 523–533.
- (17) Kataoka, K.; Miyazaki, H.; Bunya, M.; Okano, T.; Sakurai, Y. *J. Am. Chem. Soc.* **1998**, *120*, 12694–12695.
- (18) Kikuchi, A.; Suzuki, K.; Okabayashi, O.; Hoshino, H.; Kataoka, K.; Sakurai, Y.; Okano, T. *Anal. Chem.* **1996**, *68*, 823–828.
- (19) Waki, K.; Taijiro, S.; Sakurai, Y.; Okano, M.; Kataoka, K.; Koyama, Y.; Ishihara, S. Japanese Patent JP07062023, 1995.
- (20) Zhang, K.; Wu, X. Y. *J. Controlled Release* **2002**, *80*, 169–181.
- (21) Hoare, T.; Pelton, R. *Langmuir* **2006**, *22*, 7342–7350.
- (22) Hoare, T.; McLean, D. *J. Phys. Chem. B* **2006**, *110*, 20327–20336.
- (23) Hoare, T.; Pelton, R. *J. Colloid Interface Sci.* **2006**, *303*, 109–116.
- (24) Canadian Diabetes Association, 2005.
- (25) Hoare, T.; Pelton, R. *Macromolecules* **2004**, *37*, 2544–2550.

MA062254W